Contents lists available at http://qu.edu.iq

Al-Qadisiyah Journal for Engineering Sciences

Journal homepage: https://qjes.qu.edu.iq

3D-Numerical simulation of free convection inside a cubical cavity filled with non Newtonian-Bingham fluid

Mohammed Keddar [1]*, Belkacem Draoui [1], Brahim Mebarki [1] ⓘ *Marc Medale [2]* ⓘ *and Kada Benhanifia[1]* ⓘ

[1] *Laboratory of Arid Zones Energetic - (ENERGARID), Faculty of Technology, University of Tahri Mohamed Bechar, BP 417 (08000), Bechar, Algeria*
[2] *Université Aix-Marseille, Polytech Marseille, Dépt Mécanique Energétique Laboratoire IUSTI, UMR 7343 CNRS-Université Aix-Marseille Technopole de Chateau- Gombert, 5 rue Enrico Fermi 13453 MARSEILLE, Cedex 13,FRANCE*

ARTICLE INFO

ABSTRACT

This work focuses on a numerical study of natural convection of a non-Newtonian viscoplastic fluid within a cubic enclosure. The viscoplastic behavior is described by the Bingham model. The considered three-dimensional convective flow is confined within a cavity, subjected to a horizontal temperature gradient, where the vertical walls have two imposed temperatures while the rest of the walls are adiabatic. The Navier-Stokes equations, along with the mass and energy conservation equations, are numerically solved. Fluid flow and heat transfer characteristics are systematically studied over a wide range of Rayleigh number Ra (10^3 - 10^6) and Bingham number Bn (0 - 20). Finally, comparisons were made with previous results obtained in two dimensions in order to analyze the existence of a three-dimensional effect on the flow of the Bingham fluid. The results shows that the Nusselt number decreases with the increase of the Bingham number, and for the large values of the latter the heat transfer is done by conduction. It is also noteworthy that the critical Bn of the 2D model is higher than that of the 3D model, which confirms the existence of the three-dimensional effect. This is attributed to the presence of a wall along the Z axis which hinders and limits the flow of fluid within the enclosure.

1. Introduction

Viscoplastic fluids, defined by a yield stress τ_y, are known to exhibit a complicated transition between solid and fluid behavior. If the material is not sufficiently strained, i.e. less than the yield stress, it does not flow and acts as a solid. It flows with shear-thinning behavior above the yield stress. The inelastic Bingham [1], Herschel-Bulkley [2] and Casson [3-4]models are the most often employed for characterizing viscoplastic fluids. The Bingham model is the most basic approach for dealing with yield stress and it is the most commonly utilized model in theoretical and numerical

investigations due to its relative simplicity. However, the Bingham model is unrealistic. The majority of real materials behave like shear-thinning yield stress fluids like the Herschel-Bulkley or Casson fluids. The Casson model is now being utilized in the food industry[5-6]specifically by the International Office of Cocoa and Chocolate to describe the rheological behavior of chocolate. In addition, the Casson model is frequently used in medicine to match blood rheology[7-8] .The buoyancy-driven heat convection inside an enclosure has been widely investigated during the last

---

* Corresponding author.
 E-mail address: *keddar.mohammed@univ-bechar.dz (Mohammed Keddar)*

Nomenclature:

Cp	Heat capacity (J/kg K)	*Greek symbols*		
g	gravity (m/ s^2)	$\dot{\gamma}$	Shear rate (s^{-1})	
h	Height	$\dot{\gamma}_c$	Critical shear rate (s^{-1})	
k	Consistency	β	Thermal expansion coefficient (T^{-1})	
L	Domain length	λ	Thermal conductivity (W/m ^{0}C)	
p	Pressure(p)	θ	Temperature	
T	Temperature	μ	Plastic viscosity (Pa.s)	
Tp	Hot temperature	μ_a	Apparent viscosity (Pa.s)	
Tc	Cold temperature	π	Pi	
U,v,w	Velocity vector component	ρ	Volumic mass (Kg/m^3)	
X, y ,z	Cartesian coordinates			
Pr	Prandtl Number	Ra	Rayleigh Number	
Gr	Grashof Number	Bn	Bingham Number	
Nu	Nusselt Number			

several decades[9-11] .Natural convection in an enclosure [12-14]may be seen in various applications such as electronic equipment cooling, building cooling and heating, solar heaters, energy drying processes etc. The most classical case is a differentially heated cavity filled with Bingham Fluids, where the vertical walls have different temperatures while the other walls (top and bottom) are adiabatic. Vikhansky [15] investigated the flow of Bingham liquid inside a rectangular cage. The top and lower walls are thought to be adiabatic, whereas the lateral walls preserve temperature consistency. They discovered that convection occurs when the temperature difference exceeds a crucial threshold. Boutra and al.[16] numerically studied unsustainable free convection for a Bingham fluid that entirely fills a square cavity, examining the impact of Rayleigh values, Prandtl quantities, and the Viscoplasticity parameter given by the Bingham number. The vertical sides are kept at a constant temperature, whereas the horizontal walls are supposed to be adiabatic. They claimed that changes in Rayleigh, Prandtl, and Bingham quantities had a significant influence on heat flow. Fazli and al.[17] utilized Bingham's model fluid to investigate the effect of elastic stress on free convection between two vertical plates. The flow was unidirectional (1D), and they used the Boussinesq approximation. They investigate the answer, which gets quite complex when. The fluid flow stagnates, and the $Bn > Bn_{cr} = 1/16$ conduction is a prominent phenomenon. Sairamu and al.[18] reported free convection of Viscoplastic fluid in "the Bingham fluids model," and the gap is heated by the inner cylinder positioned in the middle. The study included a wide range of important characteristics, including Rayleigh quantity, Prandtl quantity, and Viscoplasticity parameters. They found that increasing the Bingham parameter value lowered the heat transmission rate. It was also revealed that the Nusselt amount has a very low reliance on Prandtl, which is reflected in the Rayleigh number expression. Keyfati[18], [19] quantitatively investigated the free double-diffusion, convective generation, and entropy of the Bingham liquid in an open and inclined enclosure. The mass transference analysis, which takes into account the Soret and Dufour components as well as the tilting effect, is unique to these papers. While the results from Ref.[21] [20] revealed that increasing Rayleigh numbers accelerates fluid flow inside the enclosure. According to Keyfati[19][21], increasing the Rayleigh number value improves heat and mass transport, while increasing the tilt angles reduces entropy formation. The data reveal that high Rayleigh and Darcy values lead to an increase in heat transfer. Increasing the Bingham number (viscoplasticity parameters) reduces the heat flow within the enclosure. Paulo and al. [22] numerically solved the free convection of a yield stress liquid within a chamber with various

barriers, and the vertical walls were differently heated due to the yield stress behavior. It is noted that increasing the viscoplasticity parameter has a substantial effect on slowing the circulation of flow inside the cavity, hence influencing the heat transfer rate. Turan and al. [23], [24] carried out 2D simulations of free laminar convection within the hollow. The investigation was conducted on several Newtonian and non-Newtonian fluids (Bingham fluid model) heated differently from the sidewalls for various reasons. They discovered that the Nusselt values for Bingham fluid are lower than those for Newtonian fluid due to the weaker transport via convection in the case of Bingham fluid. Hassan and al [25] investigated the hydro-thermal flow behavior of viscoplastic fluid (Bingham model) inside a rectangular cavity using both computational and experimental methods. This chamber is heated at its bottom wall, with the side walls serving as the cooled boundary. They discovered that, unlike in the isothermal situation, convection flow weakens with continuous heat inflow. Abderrahmane and al. [26] investigated numerically free convection inside a square enclosure differentially heated and containing Herschel-Bulkely fluid, examining the influence of Prandtl and Rayleigh values on the fluid's rheological structure. The vertical wall sides are adjusted to various temperatures, while the horizontal side wall is insulated. The working fluid is identified by its rheological index (n) and yield stress (τ_y). Variations in Rayleigh, Bingham, Prandtl, and flow index have an impact on thermal structure. Huilgol and al. [27] investigated free convection in a square cavity with vertical differential heating and a viscous fluid. This experiment used different Rayleigh, Prandtl, and Bingham numbers. The data show that heat transmission increases as Rayleigh numbers climb. However, raising the viscoplasticity parameter reduces the heat transfer rate; for further details, see Ref[28] . Mebarki and al [29]examined a steady-state laminar of free convection in a square cavity with differently heated side walls. The cavity is immersed in a viscoplastic liquid of the Bingham prototype. The horizontal walls are assumed to be adiabatic and the vertical wall presents two different sinusoidal spatial temperature profiles with different phases and amplitudes. The hydro-thermal features are systematically analyzed via a broad choice of Rayleigh number Ra, Bingham number Bn, Prandtl numbers Pr, amplitude ratio ε, phase difference π and flow index n. It has been observed that average Nusselt numbers grow with increasing Rayleigh numbers and drop with increasing Bingham quantity, since heat transition occurs primarily due to thermal conductivity. The rise in the phase difference suggests an upsurge in heat transference, as the impact of the phase shift on the Nusselt. The thermal flow rate is bigger in $\varepsilon = 1$ than in the other cases. Other works has been done with non-uniform temperature

profiles, but in different configurations than the latter (RBC), where the enclosure is filled with Bingham fluid and the horizontal walls have been subjected to sinusoidal temperatures, while the vertical walls are adiabatic see refs [30,31]. In the most published work, the simultaneous impact on heat transfer and flow patterns of boundary restrictions and the nature of non-Newtonian fluids in a 2D confined space, however this study aims to numerically investigate hydrothermal flow of the Bingham type viscoplastic fluid in 3D in order to show the three-dimensional impact. The effects of Ra and Bn are systematically studied. However, it should be noted that in the current review, plastic viscosity and yield strength are considered to be independent of temperature.

2. Description of the mathematical model

In the case of free convective flowing in a differential heated cubical cavity, the vertical walls are subjected to temperatures, as long as the rest of the walls are adiabatic (Fig. 1). In order to make the mathematical description of the conceptual framework more manageable and straightforward and to speed up the accuracy thereof, certain approximations and simplifying assumptions are made:

- 3-D Steady–state flow.
- The non-Newtonian fluid (viscoplastic model).
- The regime is supposed to be laminar.
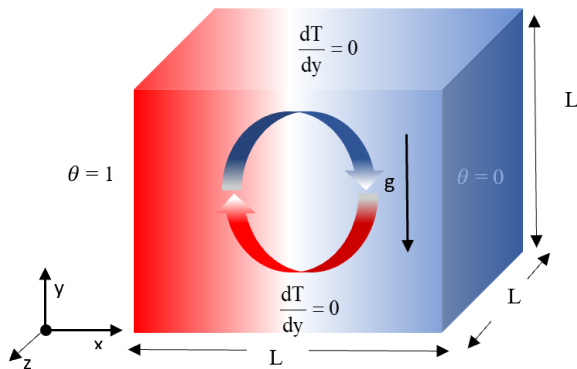- The Boussinesq approximation simplifies the pressure forces.

Figure 1. 3D model of studied problem

2.1 Governing equations

The momentum equations:

The Navier-Stokes equations system for this study is presented as follows ,[23]:

Following x:

$$u\frac{\partial u}{\partial x} + v\frac{\partial u}{\partial y} + w\frac{\partial u}{\partial z} = -\frac{\partial p}{\partial x} + Pr\left(2\frac{\partial^2 u}{\partial x^2} + \frac{\partial^2 u}{\partial y^2} + \frac{\partial^2 u}{\partial z^2} + \frac{\partial^2 v}{\partial x\partial y} + \frac{\partial^2 w}{\partial x\partial z}\right) +$$
$$\left(2\frac{\partial \mu_a}{\partial x}\frac{\partial u}{\partial x} + \frac{\partial \mu_a}{\partial y}\frac{\partial u}{\partial y} + \frac{\partial \mu_a}{\partial z}\frac{\partial u}{\partial z} + \frac{\partial \mu_a}{\partial y}\frac{\partial v}{\partial x} + \frac{\partial \mu_a}{\partial z}\frac{\partial w}{\partial x}\right) \quad (1)$$

Following y :

$$u\frac{\partial v}{\partial x} + v\frac{\partial v}{\partial y} + w\frac{\partial v}{\partial z} = -\frac{\partial p}{\partial y} + Pr\left(\frac{\partial^2 v}{\partial x^2} + 2\frac{\partial^2 v}{\partial y^2} + \frac{\partial^2 v}{\partial z^2} + \frac{\partial^2 u}{\partial x\partial y} + \frac{\partial^2 w}{\partial y\partial z}\right) +$$

$$\left(\frac{\partial \mu_a}{\partial x}\frac{\partial v}{\partial x} + 2\frac{\partial \mu_a}{\partial y}\frac{\partial v}{\partial y} + \frac{\partial \mu_a}{\partial z}\frac{\partial v}{\partial z} + \frac{\partial \mu_a}{\partial x}\frac{\partial u}{\partial y} + \frac{\partial \mu_a}{\partial z}\frac{\partial w}{\partial y}\right) + Pr.Ra.\theta \quad (2)$$

Following z :

$$u\frac{\partial w}{\partial x} + v\frac{\partial w}{\partial y} + w\frac{\partial w}{\partial z} = -\frac{\partial p}{\partial z} + Pr\left(\frac{\partial^2 w}{\partial x^2} + \frac{\partial^2 w}{\partial y^2} + 2\frac{\partial^2 w}{\partial z^2} + \frac{\partial^2 u}{\partial x\partial z} + \frac{\partial^2 v}{\partial y\partial z}\right)$$

$$+ \left(\frac{\partial \mu_a}{\partial x}\frac{\partial w}{\partial x} + \frac{\partial \mu_a}{\partial y}\frac{\partial w}{\partial y} + 2\frac{\partial \mu_a}{\partial z}\frac{\partial w}{\partial z} + \frac{\partial \mu_a}{\partial x}\frac{\partial u}{\partial z} + \frac{\partial \mu_a}{\partial y}\frac{\partial v}{\partial z}\right) \quad (3)$$

Where:

$$\begin{cases} \mu_a = K\dot{\gamma}^{n-1} + \frac{\tau_0}{\dot{\gamma}} \, si \, \tau > \tau_0 \\ \dot{\gamma} = 0(\mu_a \to \infty) \, si \, \tau \le \tau_0 \end{cases}$$

Continuity formula:

$$\frac{\partial u}{\partial x} + \frac{\partial v}{\partial y} + \frac{\partial w}{\partial z} = 0 \quad (4)$$

The energy equation:

$$u\frac{\partial \theta}{\partial x} + v\frac{\partial \theta}{\partial y} + w\frac{\partial \theta}{\partial z} = \left(\frac{\partial^2 \theta}{\partial x^2} + \frac{\partial^2 \theta}{\partial y^2} + \frac{\partial^2 \theta}{\partial z^2}\right) \quad (5)$$

The above equations became dimensionless by introducing these variables.

$$x = \frac{x^*}{L} \, , \, y = \frac{y^*}{L} \, , \, z = \frac{z^*}{L} \, , \, u = \frac{u^*L}{\alpha} \, , \, v = \frac{v^*L}{\alpha} \, , \, w = \frac{w^*L}{\alpha} \, p = \frac{p^*L}{\rho\alpha^2}$$

$$\theta = \frac{T-T_f}{T_c-T_f}$$

Left wall of the domain:

$T_c = 1, u = v = 0$

Right wall of the domain

$T_c = 0, u = v = 0$

The rest of the walls are considered adiabatic

$$\frac{dT}{dy} = 0, u = v = 0 \quad (6)$$

The Herschel-Bulkley model is described by the following equations:

$$\dot{\gamma} = 0 \qquad si \quad \tau \le \tau_0$$
$$\tau = \tau_0 + K\dot{\gamma}^n \quad si \quad \tau > \tau_0 \quad (7)$$

The Bingham model is governed by the following equations:

$$\dot{\gamma} = 0 \qquad si \quad \tau \le \tau_0$$
$$\tau = \left(\mu + \frac{\tau_0}{\dot{\gamma}}\right)\dot{\gamma} \quad si \quad \tau > \tau_0 \quad (8)$$

Dimensionless Rayleigh number:

$$Ra = \frac{\rho^2 Cpg\beta\Delta TL^3}{\mu\lambda} = GrPr \quad (9)$$

Dimensionless Grashoff number:

$$Gr = \frac{\rho^2 g\beta\Delta TL^3}{\mu^2} \quad (10)$$

Dimensionless Prandtl number:

$$Pr = \frac{\mu Cp}{\lambda} \quad (11)$$

Dimensionless Bingham number:

$$Bn = \frac{\tau_0}{\mu}\sqrt{\frac{L}{g\beta\Delta TL}} \quad (12)$$

The thermal transfer rate is analyzed by the parameter Nusselt quantity:

$$Nu = \frac{hL}{\lambda} \quad (13)$$

Where h is defined by:

$$h = \left|-\lambda\frac{\partial T}{\partial x}\right| \times \frac{1}{(T_{wall}-T_{ref})} \quad (14)$$

The Nusselt number is calculated for the studied cases to observe when rheological behavior leads to an improvement or degradation in heat

transfer rate.

3. Numerical methods

FLUENT, a commercial CFD software, provides the numerical model. Subject to the suggested boundary conditions, the conservation equations are discretized using a finite-volume technique based on the COUPLED algorithm. The second-order upwind differencing method is used to discretize the equations. Finally, the convergence requirements for solving the governing equations are regarded met when the sum of the residuals is less than 10^{-6}.

Table 1. Numerical mesh test of the Newtonian fluid for Ra $= 10^4$; Pr=7; Bn = 0.5.

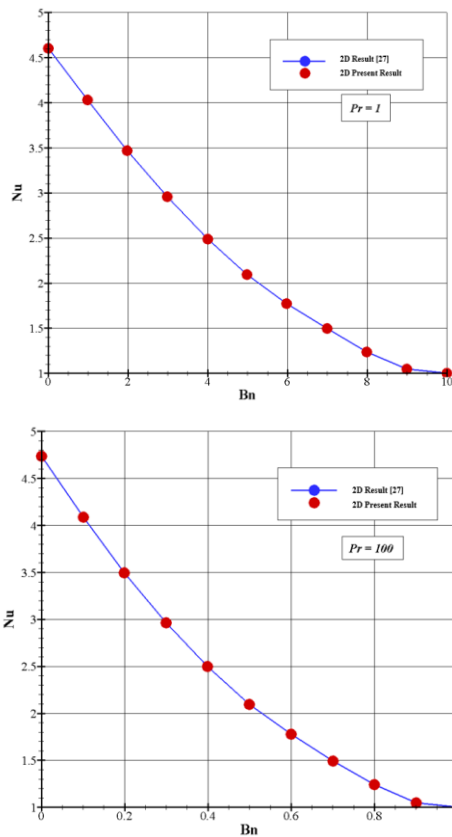| Mesh	M1	M2	M3
Grid	31×31×31	51×51×51	80×80×80
Nu	02.098	02.088	02.080
V_{max}	19.415	19.510	19.530

Figure 2. Comparison of the Nusselt obtained with those of the article [24]

3.1 Mesh test

The tested the influence of the mesh on the results for this we used three structural meshes M1(31×31×31), M2(51×51×51) and M3(80×80×80), however the results obtained from the Nusselt number are presented in

Table 1. The table show that M2 mesh (132651 Nodes, 125000 Elements) is a good compromise between precision and CPU time cost.

Table 2. Nusselt validation [27], Ra = 10^5

	Bn = 01	Bn = 03	Bn = 06	Bn = 09	Bn = 18	Bn = 27
Ref. [27]	3.303	3.263	3.083	2.898	2.402	2.143
This work	3.305	3.265	3.083	2.900	2.403	2.140
Error (%)	0.06	0.09	0.00	0.07	0.04	0.14

3.2 Validation

To validate our results, we compared them to those in the literature, namely the work of references [24] and [27]. To confirm the validation of our results, we calibrated our numerical model by comparing our Nusselt results, which includes the speeds and temperatures with the reference [24] and [27] in addition to the contours of the Isotherms and the lines of common with article [27].
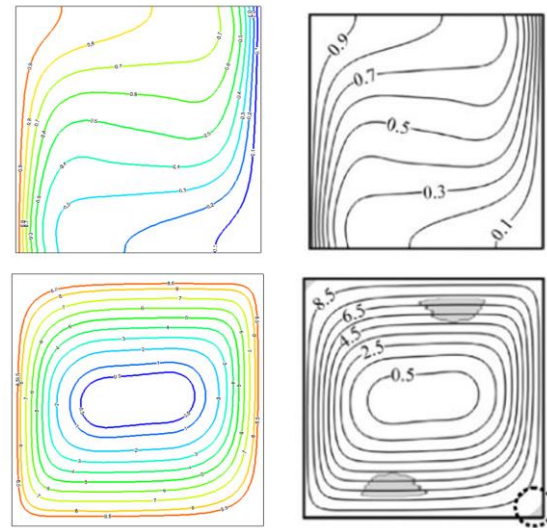

Figure 3. Comparison of isotherms (top) and streamlines (bottom) obtained with the and those of the article [24]

In Figure 2, we observe a very good agreement between our results and those found in the literature. This agreement is clearly demonstrated by the low percentage of error calculated between our results and the reference values from literary sources. In addition, the shape of the isotherms and streamlines presented in Figure 3 is identical to that shown in reference.

4. Results and discussion

In this part we will present the results obtained from three-dimensional laminar flow within a closed enclosure filled with a non-Newtonian fluid, in this case the Bingham fluid. The non-Newtonian fluid is assumed to be incompressible, the regime is assumed to be laminar, for this we have varied the Rayleigh number Ra, the Bingham number Bn, and the Prandtl number Pr.
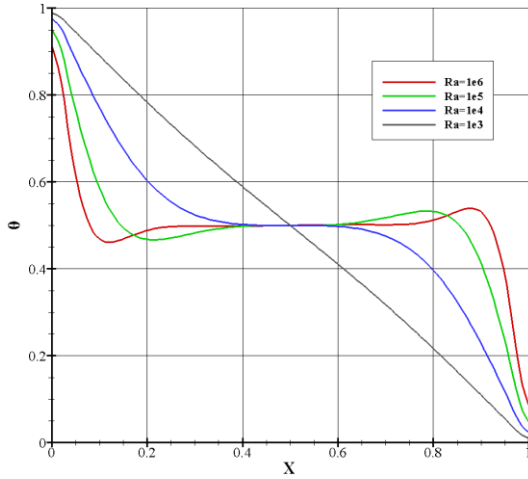
Figure 4. Newtonian fluid temperature for ; Bn = 0; Pr = 7

4.1 Effect of Rayleigh number

We notice that the Rayleigh number has a significant influence on the lines of isotherms of the Newtonian fluid which are represented in Figure 6.
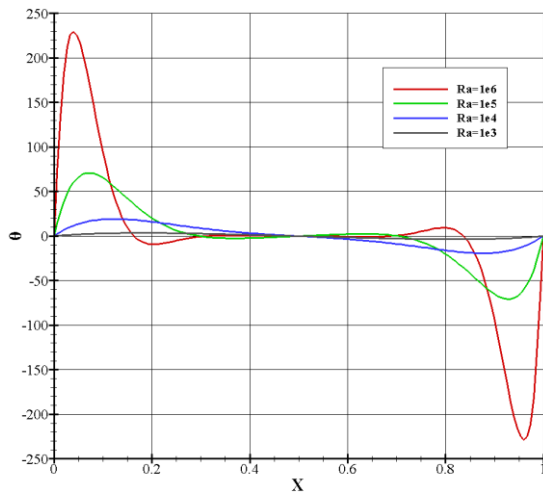

Figure 5. Newtonian fluid velocities for Bn = 0 ; Pr = 7

This observation is attributable to the increase in the dimensionless number. This number is essentially responsible for generating convection, i.e. it is the element that induces heat transfer by convection. we can clearly see this in Figures 4 and 5 which represent the dimensionless temperatures and speeds of the Newtonian fluid.

The contours of the Bingham fluid isotherms are shown in Figure 9. For a number of Ra=10^3, the isotherms are completely linear due to very low flow because the effects of buoyancy forces are dominated by viscous effects. Under these conditions, heat transfer occurs entirely by conduction through the enclosure. When the Rayleigh number increases to Ra = 10^4, the structure of the isotherms begins to change and become distorted. Obviously, at this point, convection is triggered. We can better understand if we observe the temperature and speed profiles which are indicated in Figures 7 and 8, that with the increase in the Rayleigh number the heat transfer goes from conduction to convection.
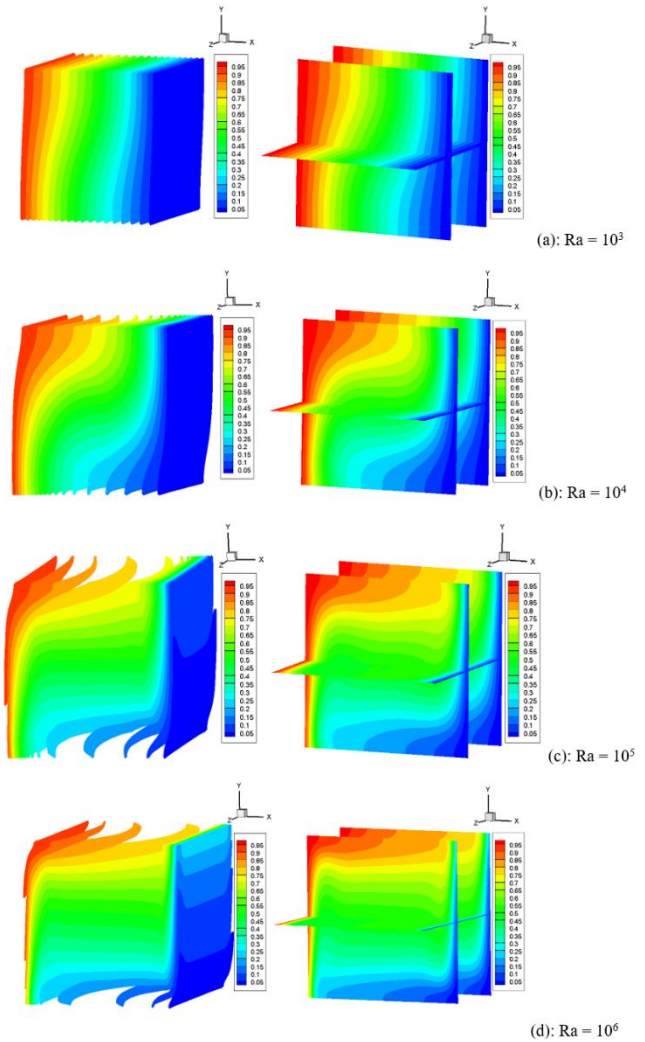

(a): Ra = 10^3

(b): Ra = 10^4

(c): Ra = 10^5

(d): Ra = 10^6

Figure 6.: Contours of the isotherms of the Newtonian fluid for Bn = 0 ; Pr = 7.
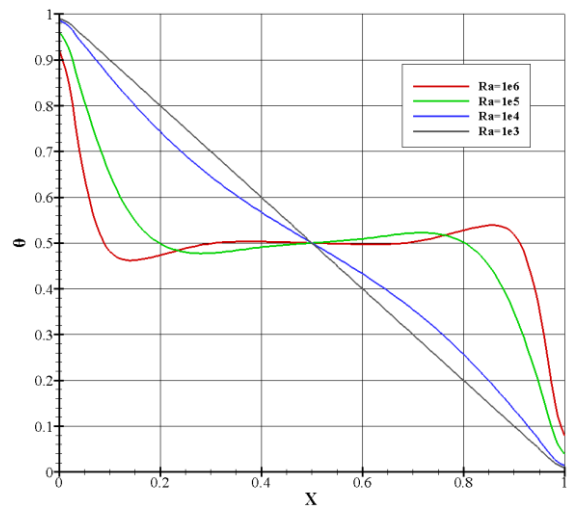
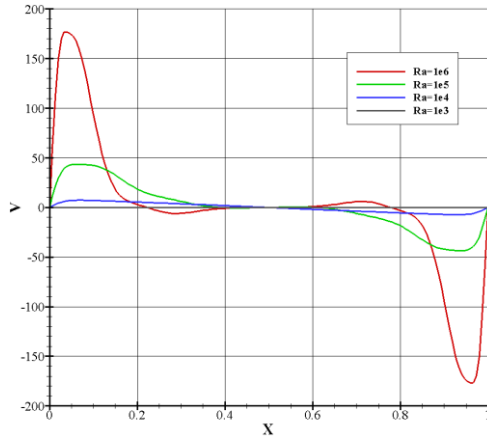**Figure 7.** Bingham fluid temperature for Bn = 0,5 ; Pr = 7

Figure 8. Bingham fluid velocities for Bn = 0,5 ; Pr = 7

(a): Ra = 10^3

(b): Ra = 10^4
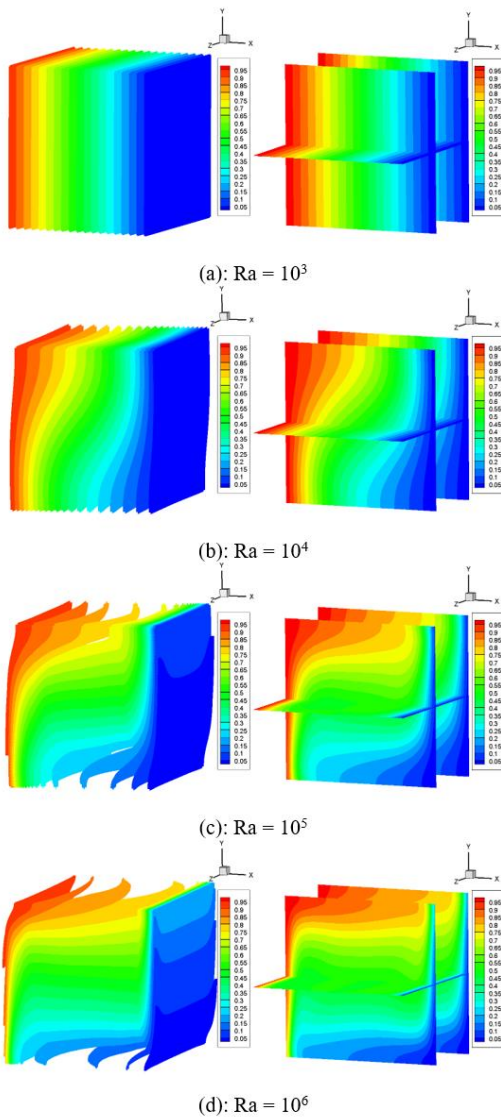

(c): Ra = 10^5

(d): Ra = 10^6

Figure 9. Isotherm contours for Bn = 0.5 ; Pr = 7.

4.2 Effect of Bingham number

For high values of the Bingham number, viscous force more readily overcomes buoyancy force, thus preventing any induced flow within the enclosure. This behavior can be better understood by comparing the contours of isotherms in Figures 12 and 15 for different values of Bn at Ra=10^4 and Ra=10^6, respectively. These figures suggest that the effects of convection within the enclosure decrease with increasing Bingham number, and the Bingham fluid begins to behave like a solid. In the absence of flow within the enclosure, heat transfer occurs through conduction. This can be better understood by examining temperature and velocity profiles shown in Figures 10, 11, 13, and 14 for Ra=10^4 and Ra=10^6, respectively, where it can be observed that increasing the Bingham number transitions heat transfer from convection to conduction.

4.3 Comparison of results obtained in 3D and 2D

In this final part, we compared the results obtained in 2D and 3D to demonstrate the existence of a three-dimensional effect.

4.3 Comparison of results obtained in 3D and 2D

In this final part, we compared the results obtained in 2D and 3D to demonstrate the existenc of a three-dimensional effect. This can be observed in Figure 16, which depicts the flow velocity within the enclosure, and in Figure 17, which illustrates the Nusselt number incorporating velocities and temperatures.The evolution of the results reveals that increasing the Bingham number leads to a decrease in flow velocity until it reaches nullification, while the Nusselt number decreases until it reaches a value of 1. This indicates that the dominant mode of heat transfer shifts towards conduction. Finally, it can be observed that the critical Bingham number of the 2D model is higher than that of the 3D model, which proves the existence of the three-dimensional effect caused by the wall along the Z-axis that blocks and prevents fluid flow within the enclosure.
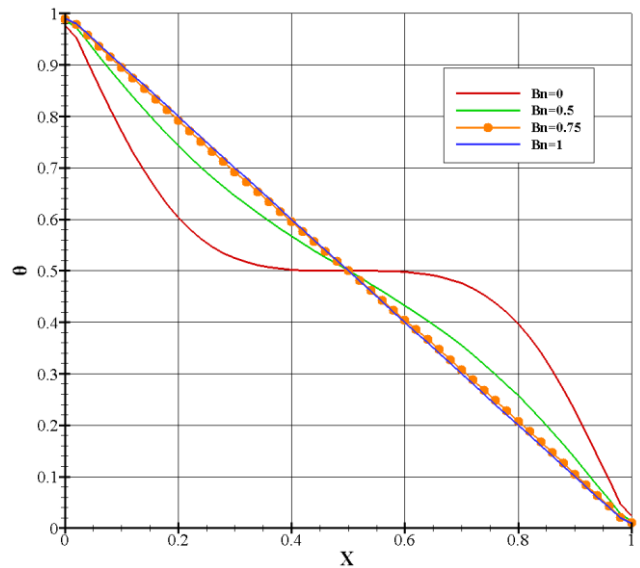

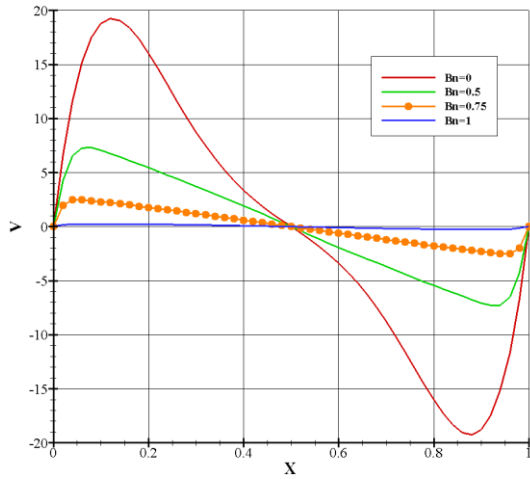**Figure 10**. Temperature distribution for Ra = 10^4 ; Pr = 7

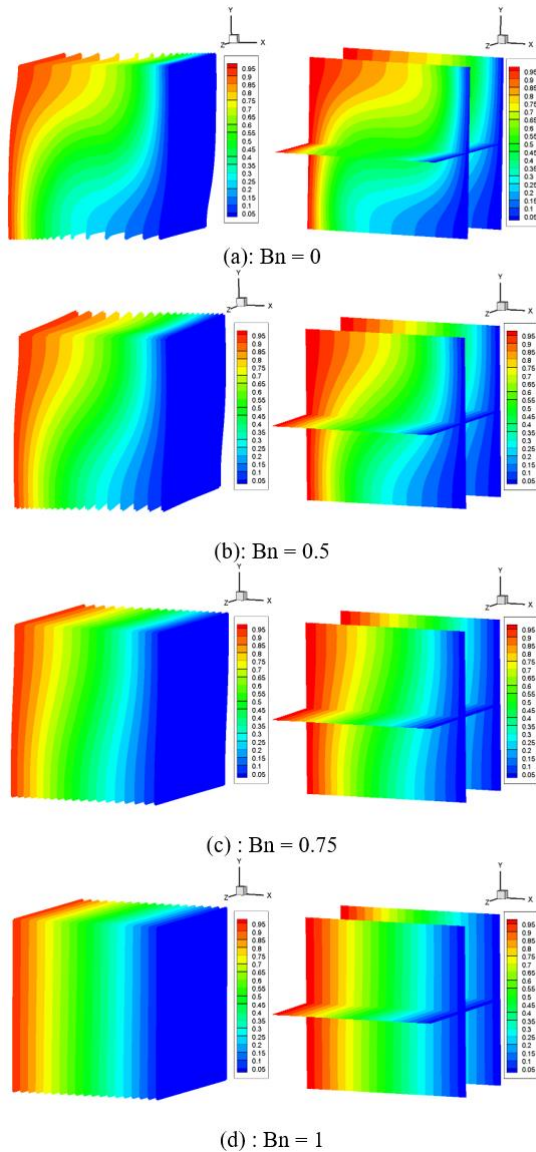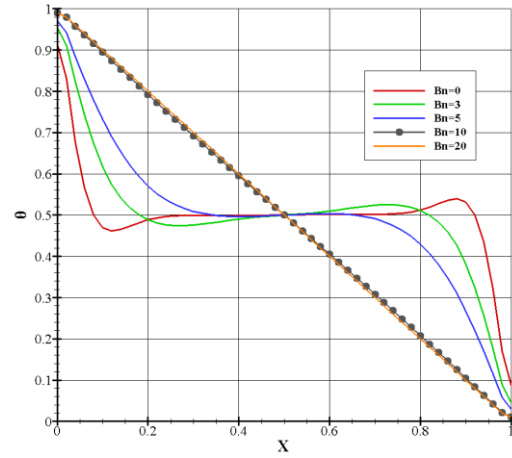**Figure 11.** Velocity distribution for $Ra = 10^4$; $Pr = 7$

Figure 13. Temperature distribution for $Ra = 10^6$; $Pr = 7$

(a): Bn = 0

(b): Bn = 0.5
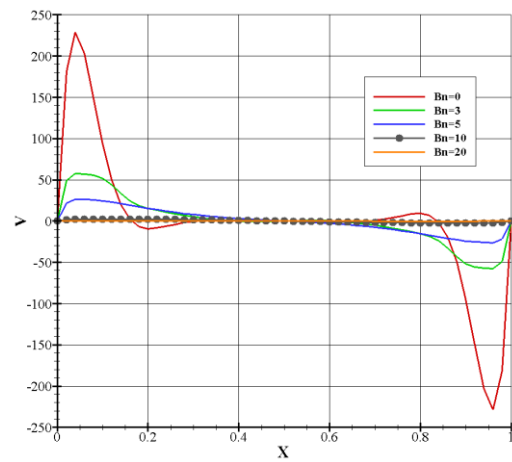
Figure 14. Velocity distribution for $Ra = 10^6$; $Pr = 7$

(c) : Bn = 0.75

(d) : Bn = 1

Figure 12. Isotherm Contours inside the cavity for $Ra = 10^4$; $Pr = 7$.

(a) : |Bn| = 0

(b) : Bn = 3
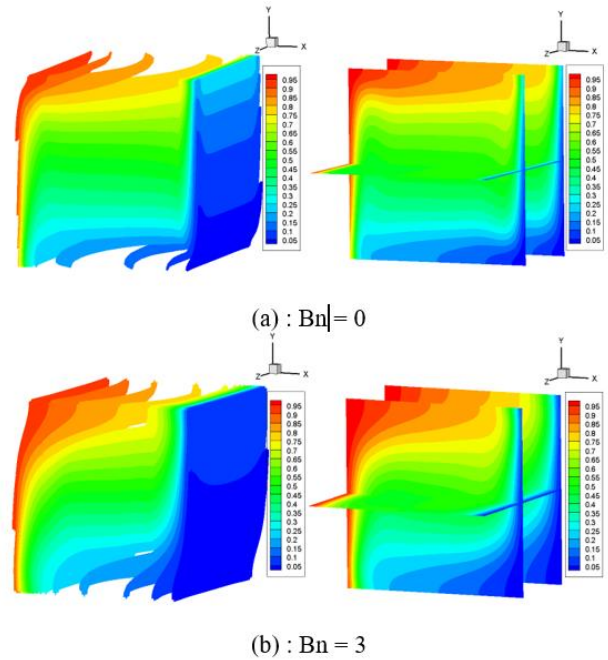
Figure 15. isotherms Contours of Bingham fluid for $Ra = 10^6$; $Pr = 7$.

(c) : Bn = 5

(d) : Bn = 10

(e) : Bn = 20

Figure 15 (Continued). isotherms Contours of Bingham fluid for Ra = 10^6; Pr = 7.
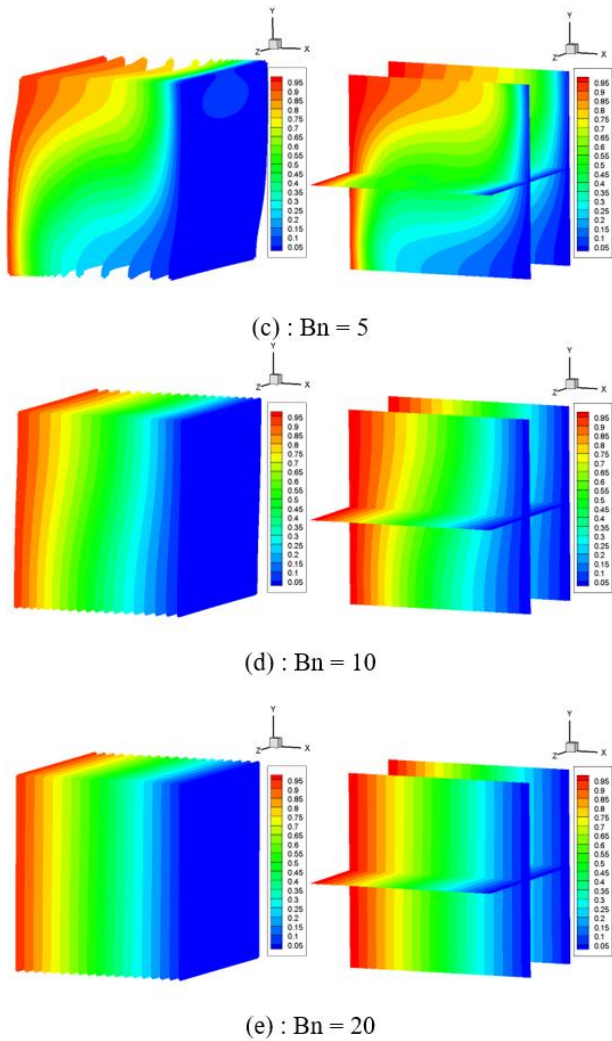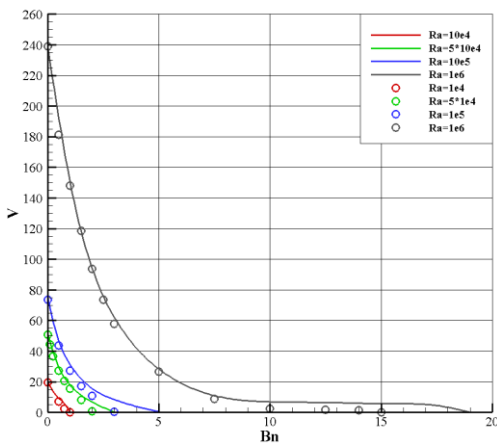

Figure 16. Comparison of velocity distribution between 2D (-) and 3D (o) models .

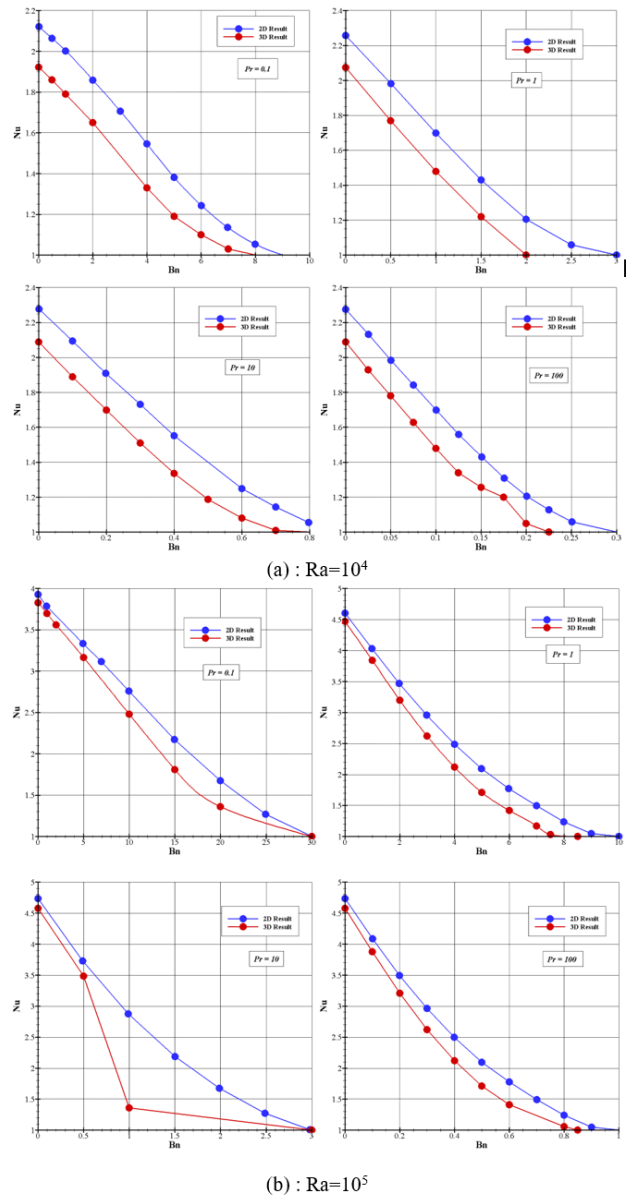(a) : Ra=10^4

(b) : Ra=10^5

Figure 17. Comparison of Nusselt number for different model 2D and 3D.

4 Conclusion

To conclude, the results obtained from our investigation into three-dimensional laminar flow within a closed enclosure filled with a non-Newtonian Bingham fluid, under the assumption of steady-state conditions, yield several key insights: Impact of Non-Dimensional Parameters on Heat Transfer: We have systematically analyzed the effects of the Rayleigh, Prandtl, and Bingham numbers on heat transfer within the system. The findings reveal that an increase in the Bingham number corresponds to a decrease in the flow velocity, ultimately leading to a cessation of flow. Concurrently, the Nusselt number diminishes until it approaches a value of 1. This trend signifies a transition in the predominant heat transfer mechanism from convective to conductive heat transfer, highlighting the influence of fluid rheology on thermal performance. Comparison of Critical Bingham Numbers: The analysis indicates that the critical Bingham number for the two-dimensional (2D) model is higher than that of the three-

dimensional (3D) model. This discrepancy underscores the presence of a significant three-dimensional effect introduced by the enclosure's geometry along the Z-axis. Specifically, the enclosure's walls interact with the flow, obstructing and impeding fluid movement more profoundly in three dimensions compared to two. This finding confirms that three-dimensional effects play a crucial role in accurately capturing the fluid dynamics and heat transfer characteristics in the enclosure. In summary, our study highlights the critical role of dimensionality in the modeling of non-Newtonian fluid flows and their thermal behavior, providing a more nuanced understanding of how Bingham fluids behave under different conditions.

Authors' contribution

All authors contributed equally to the preparation of this article.

Declaration of competing interest

The authors declare no conflicts of interest.

Data availability

The data that support the findings of this study are available from the corresponding author upon reasonable request

.

REFERENCES

[1] E. C. Bingham, *An investigation of the laws of plastic flow*, no. 278. US Government Printing Office, 1917.

[2] W. H. Herschel and R. Bulkley, "Calibration of the Buret consistometer," *Ind Eng Chem*, vol. 19, no. 1, pp. 134–139, 1927.

[3] M. Aneja, A. Chandra, and S. Sharma, "Natural convection in a partially heated porous cavity to Casson fluid," *International Communications in*

[4] *Heat and Mass Transfer*, vol. 114, p. 104555, 2020.

[5] K. Benhanifia *et al.*, "Investigation of mixing viscoplastic fluid with a modified anchor impeller inside a cylindrical stirred vessel using Casson–Papanastasiou model," *Sci Rep*, vol. 12, no. 1, pp. 1–19, 2022.

[6] V. De Graef, F. Depypere, M. Minnaert, and K. Dewettinck, "Chocolate yield stress as measured by oscillatory rheology," *Food Research International*, vol. 44, no. 9, pp. 2660–2665, 2011.

[7] M. A. Rao and M. A. Rao, "Flow and functional models for rheological properties of fluid foods," *Rheology of fluid, semisolid, and solid foods: Principles and applications*, pp. 27–61, 2014.

[8] F. Ali, N. A. Sheikh, I. Khan, and M. Saqib, "Magnetic field effect on blood flow of Casson fluid in axisymmetric cylindrical tube: A fractional model," *J Magn Magn Mater*, vol. 423, pp. 327–336, 2017.

[9] M. W. S. Khan and N. Ali, "Theoretical analysis of thermal entrance problem for blood flow: an extension of classical Graetz problem for Casson fluid model using generalized orthogonality relations," *International Communications in Heat and Mass Transfer*, vol. 109, p. 104314, 2019.

[10] M. S. Sadeghi, T. Tayebi, A. S. Dogonchi, M. K. Nayak, and M. Waqas, "Analysis of thermal behavior of magnetic buoyancy-driven flow in ferrofluid–filled wavy enclosure furnished with two circular cylinders," *International Communications in Heat and Mass Transfer*, vol. 120, p. 104951, 2021.

[11] M. A. Ghurban, K. Al-Farhany, and K. Benhanifia, "Effects of Fin on mixed convection heat transfer in a vented square cavity: A numerical study," 2023.

[12] A. M. Barik and K. Al-Farhany, "Numerical investigation of the effect of baffle inclination angle on nanofluid natural convection heat transfer in a square enclosure," *Al-Qadisiyah Journal for engineering sciences*, vol. 12, no. 2, pp. 61–71, 2019.

[13] Q.-H. Deng and J.-J. Chang, "Natural convection in a rectangular enclosure with sinusoidal temperature distributions on both side walls," *Numeri Heat Transf A Appl*, vol. 54, no. 5, pp. 507–524, 2008.

[14] A. Bejan, "Convection heat transfer, Wiley," *New York*, 1984.

[15] G. de Vahl Davis, "Natural convection of air in a square cavity: a bench mark numerical solution," *Int J Numer Methods Fluids*, vol. 3, no. 3, pp. 249–264, 1983.

[16] A. Vikhansky, "On the onset of natural convection of Bingham liquid in rectangular enclosures," *J Nonnewton Fluid Mech*, vol. 165, no. 23–24, pp. 1713–1716, 2010.

[17] A. Boutra, Y. K. Benkhalla, D. E. Ameziani, and N. Labsi, "Etude numérique du transfert de chaleur pour un fluide de Bingham dans une cavité carrée en mode de convection naturelle instationnaire," in *CFM 2011-20ème Congrès Français de Mécanique*, AFM, Maison de la Mécanique, 39/41 rue Louis Blanc-92400 Courbevoie, 2011.

[18] I. Karimfazli and I. A. Frigaard, "Natural convection flows of a Bingham fluid in a long vertical channel," *J Nonnewton Fluid Mech*, vol. 201, pp. 39–55, 2013.

[19] M. Sairamu, N. Nirmalkar, and R. P. Chhabra, "Natural convection from a circular cylinder in confined Bingham plastic fluids," *Int J Heat Mass Transf*, vol. 60, pp. 567–581, 2013.

[20] G. H. R. Kefayati, "Lattice Boltzmann method for natural convection of a Bingham fluid in a porous cavity," *Physica A: Statistical Mechanics and Its Applications*, vol. 521, pp. 146–172, 2019.

[21] G. H. R. Kefayati, "Double-diffusive natural convection and entropy generation of Bingham fluid in an inclined cavity," *Int J Heat Mass Transf*, vol. 116, pp. 762–812, 2018.

[22] F. Danane, A. Boudiaf, O. Mahfoud, S.-E. Ouyahia, N. Labsi, and Y. K. Benkhalla, "Effect of backward facing step shape on 3D mixed convection of Bingham fluid," *International journal of thermal sciences*, vol. 147, p. 106116, 2020.

[23] P. R. M. Santos, A. Lugarini, S. L. M. Junqueira, and A. T. Franco, "Natural convection of a viscoplastic fluid in an enclosure filled with solid obstacles," *International Journal of Thermal Sciences*, vol. 166, p. 106991, 2021.

[24] O. Turan, R. J. Poole, and N. Chakraborty, "Aspect ratio effects in laminar natural convection of Bingham fluids in rectangular enclosures with differentially heated side walls," *J Nonnewton Fluid Mech*, vol. 166, no. 3–4, pp. 208–230, 2011.

[25] O. Turan, N. Chakraborty, and R. J. Poole, "Laminar natural convection of Bingham fluids in a square enclosure with differentially heated side walls," *J Nonnewton Fluid Mech*, vol. 165, no. 15–16, pp. 901–913, 2010.

[26] M. A. Hassan, M. Pathak, M. K. Khan, and N. H. Khan, "Natural convection of viscoplastic fluids in an enclosure with partially heated bottom wall," *International Journal of Thermal Sciences*, vol. 158, p. 106527, 2020.

[27] H. Abderrahmane, D. Salah-Eddine, and N. Ait-Messaoudene, "Natural convection for a Herschel-Bulkely fluid inside a differentially heated square cavity," *International Journal of Mechanics and Energy (IJME)*, vol. 6, no. 1, pp. 7–15, 2018.

[28] R. R. Huilgol and G. H. R. Kefayati, "Natural convection problem in a Bingham fluid using the operator-splitting method," *J Nonnewton Fluid Mech*, vol. 220, pp. 22–32, 2015.

[29] S. Bijjam and A. K. Dhiman, "CFD analysis of two-dimensional non-Newtonian power-law flow across a circular cylinder confined in a channel," *Chem Eng Commun*, vol. 199, no. 6, pp. 767–785, 2012.

[30] B. Mebarki *et al.*, "A CFD examination of free convective flow of a non-Newtonian viscoplastic fluid using ANSYS Fluent," *Arabian Journal of Chemistry*, vol. 16, no. 12, p. 105309, 2023.

[31] Mohammed, K., Belkacem, D., Brahim, M., & Marc, M. (2023). Rayleigh Benard convection of Bingham fluid in a square enclosure with sinusoidal temperatures. *Proceedings of the 9th World Congress on Mechanical, Chemical, and Material Engineering*, 1–8. https://doi.org/10.11159/htff23.144

[32] Mohammed, K., Belkacem, D., Brahim, M., & Marc, M. (2023). Natural Rayleigh Benard Convection of Bingham Fluid in Enclosure Cavity with Sinusoidal Profiles. *International Conference on Fluid Flow, Heat and Mass Transfer*, *127*. https://doi.org/10.11159/ehst23.127